Tailoring the fatigue response of flax FRP composites by exploiting Micro-structural re-arrangements and auxiliary loading sequences

Perruchoud, Valentin; Alderliesten, René; Mosleh, Yasmine

DOI
10.1016/j.compositesa.2025.109180

Publication date
2025

Document Version
Final published version

Published in
Composites Part A: Applied Science and Manufacturing

Citation (APA)
Perruchoud, V., Alderliesten, R., & Mosleh, Y. (2025). Tailoring the fatigue response of flax FRP composites by exploiting Micro-structural re-arrangements and auxiliary loading sequences. *Composites Part A: Applied Science and Manufacturing*, *199*, Article 109180. https://doi.org/10.1016/j.compositesa.2025.109180

Composites: Part A 199 (2025) 109180

Contents lists available at ScienceDirect

Composites Part A

journal homepage: www.elsevier.com/locate/compositesa

Tailoring the fatigue response of flax FRP composites by exploiting Micro-structural re-arrangements and auxiliary loading sequences

Valentin Perruchoud [a,*], René Alderliesten [b], Yasmine Mosleh [a]

[a] Biobased Structures and Materials, Faculty of Civil Engineering and Geosciences, Delft University of Technology, Stevinweg 1, 2628 CN Delft, the Netherlands
[b] Aerospace Structures and Materials, Faculty of Aerospace Engineering, Delft University of Technology, Kluyverweg 1, 2629HS Delft, the Netherlands

ARTICLE INFO

Keywords:
Flax fibre polymer composite
Interrupted fatigue
Auxiliary loading sequence
Microstructural re-arrangements

ABSTRACT

Fatigue behaviour of fibre-reinforced polymers (FRPs) in laboratory is typically evaluated under continuous loading. However, real-life loading scenarios of structures, e.g. bridges or wind turbine blades, often involve complex histories. These include fatigue loading interruptions, creep, combined creep-fatigue, or peak loads. While such variations may be negligible for elastic carbon and glass fibres, the viscoelastic nature of flax fibres makes them sensitive to complex loading patterns, potentially affecting the fatigue performance. Moreover, some flax preforms are made of twisted yarns, adding one more level of complexity to the hierarchical microstructure of flax FRP laminates. However, the effects of auxiliary loading sequences and the microstructure at the yarn/fibre levels, on the fatigue behaviour of flax FRPs remain largely unexplored. Therefore, this paper pioneers investigation of these effects, giving insights on how to exploit microstructural re-arrangements, preloading, and load interruptions to tailor fatigue response of flax FRPs in comparison to glass FRPs. The findings reveal that the yarn un-twisting significantly influences fatigue behaviour, leading to a doubling of strain accumulation, and dynamic stiffness increment, compared to flax FRPs with straight fibres.

Additionally, the pre-creeping and fatigue interruptions were found to substantially impact fatigue life, particularly in laminates with yarn twist, leading to a 1.7-fold increase due to interruptions and a threefold increase following pre-creeping. The latter also yielding a near-elimination of strain accumulation. Therefore, pre-creeping is proposed as an effective strategy to reduce in-service strain accumulation and extend fatigue life in predominantly UD flax FRPs with twisted yarns.

1. Introduction

The reliance on synthetic composites such as glass fibre-reinforced polymer composites (glass FRPs) in high-performance structural applications such as bridges and wind turbine blades has raised significant concerns due to the depletion of fossil resources and the environmental impacts associated with their production and disposal. As an alternative, natural lignocellulosic fibres such as flax and hemp have gained interest due to their renewable nature, biodegradability, low environmental footprint, low embodied energy, clean manufacturing, and high specific stiffness potentially making them suitable for structural applications particularly where stiffness is the primary design criterion. However, with the adoption of natural fibres such as flax as potential replacement for glass fibres in FRP structures, a comprehensive knowledge of their long-term behaviour under complex loads and environmental conditions is crucial.

Real world FRP structures such as wind turbine blades and bridges often undergo complex irregular loading scenarios. These include creep, fatigue, and interrupted fatigue loads, which can occur sequentially and/or simultaneously. These complex loading scenarios induce time-dependent mechanical responses of FRP materials mainly due to the viscoelastic nature of polymeric matrices. Due to the viscoelasticity of the matrix, creep phenomenon can occur during cycling loading of angle-ply laminates, affecting damage patterns and their evolution and ultimately fatigue response [1–4]. Creep is also known to affect the fatigue response of those materials when applied as a preloading that can result in an increase of fatigue life and fatigue failure strain [5]. A practical illustration of this approach is found in the flax FRP bridge in Ritsumasyl, the Netherlands, where a pre-creeping stage was implemented as a form of preloading prior to installation [6]. In this specific

* Corresponding author.
E-mail address: V.P.Perruchoud@tudelft.nl (V. Perruchoud).

https://doi.org/10.1016/j.compositesa.2025.109180
Received 20 May 2025; Received in revised form 2 July 2025; Accepted 13 July 2025
Available online 14 July 2025

example, this strategy aimed to reduce subsequent in-service creep deformation due to the viscoelasticity of the flax fibres.

Furthermore, viscoelasticity affects fatigue response in case of fatigue interruptions with stiffness recovery during the interruptions delaying damage propagation and stress relaxations, leading to potential increase of fatigue life [7]. For flax FRPs, the viscoelastic response can be more significant compared to synthetic glass and carbon FRPs. In contrast with elastic carbon and glass fibres, flax fibres possess a viscoelastic nature themselves [8,9]. Consequently, in structures made of flax FRPs, both fibre and matrix could contribute to viscoelastic response of the composite.

Viscoelastic behaviour in flax fibre composites stems from flax fibre polymeric constituents (such as hemicellulose, lignin, and amorphous cellulose [3,4,8,10]) and the complex hierarchical microstructure of flax FRP laminates across multiple length scales (macro, meso, and micro) as shown in Fig. 1 illustrating a UD flax FRP laminate containing flax twisted yarns. At the microscale, the technical fibres are bundles of elementary fibres held together by pectin-rich middle lamella layers [1,2]. The elementary fibres comprise of concentric primary and secondary cell walls with a hollow central channel (lumen). The secondary cell wall consists of three sub-layers: S1, S2, S3 [1]. The S2 layer, the thickest and most critical for mechanical properties of the fibres, contains highly crystalline cellulose microfibrils embedded in a matrix of lignin and hemicellulose, which are helically arranged at a tilt angle of approximately 5 to 10° to the fibre axis, imparting high tensile strength and stiffness [11–14].

The secondary cell wall consists of three sub-layers: S1, S2, S3 [15]. The S2 layer, the thickest and most critical for mechanical properties of the fibres, contains highly crystalline cellulose microfibrils embedded in a matrix of lignin and hemicellulose, which are helically arranged at a tilt angle of approximately 10° to the fibre axis, imparting high tensile strength and stiffness [12,14,16–18].

At the *meso*-scale, flax fibre preforms utilised for composite manufacturing are often made of yarns in which a degree of twist is applied on the fibre bundles to improve the yarn strength [19,20]. This twist angle of the fibre bundles with respect to the yarn axis which typically coincides with one of the main loading axes of the composite, may lead to re-alignment mechanisms upon loading due to unravelling of the twist, affecting the fatigue response. Such re-alignment mechanisms are typically absent in glass and carbon composites, as the continuity of these synthetic fibres eliminates the need for twisting to maintain preform integrity. In this context, the application of preloading as a form of pre-straining (short-term loading) was investigated in both glass FRP composites with straight fibres and flax FRPs with twisted flax yarns [21]. An enhancement in dynamic stiffness and a reduction in strain accumulation were observed in the flax FRP, but not in the glass FRP. This improvement was partially attributed to the fibre alignment mechanisms enabled by the twisted structure of the flax yarns.

While the fatigue behaviour of flax FRPs is known to be influenced by their inherent microstructural heterogeneity and viscoelastic properties, comprehensive investigations into these aspects remain limited. In particular, the combined effects of yarn twist and pre-loading or loading interruptions on fatigue performance, specifically in terms of strain accumulation, dynamic stiffness degradation, and overall fatigue life, have not yet been systematically explored in the existing literature. Developing an understanding of these phenomena is essential for the reliable structural integration of flax FRPs.

Given the limited understanding of how auxiliary loading sequences and microstructural characteristics influence the fatigue performance of natural fibre composites, this study addresses the fatigue behaviour of flax FRPs in comparison to conventional glass FRPs. Particular attention is given to the effects of preloading and load interruptions, as well as fibre architecture. In this context, the distinction between aligned fibres and twisted yarns is considered in relation to their influence on stiffness, strain accumulation, and fatigue life. It is hypothesised that both the occurrence of preloading or loading interruption events and the microstructural arrangement of the reinforcement, especially at the yarn scale, play a decisive role in governing the fatigue response. To test this, $[0/90/0]_S$ flax/epoxy laminates reinforced with either aligned fibres preforms (FlaxTape) or twisted yarns preforms (Amplitex) were subjected to three distinct types of loading: (a) pre-straining with quasi-static loading followed by fatigue, (b) pre-creeping with long-term loading followed by fatigue, and (c) fatigue with intermittent interruptions, simulating operational variability. Strain accumulation, stiffness degradation, and fatigue life were monitored and compared against a [0/90/0] glass/epoxy laminate, used as a reference material with elastic reinforcement. To further elucidate the role of fibre architecture, microscopy analysis was conducted on the flax laminates post-fatigue to examine damage patterns and mechanisms associated with fibre/yarn re-orientation.

2. Materials and methods

2.1. Composite laminates

2.1.1. Architecture

Two types of flax fabrics were chosen to have straight fibres and twisted fibres reinforcement to study the effect of different fibre arrangement. The flax FRP laminates with straight fibres were manufactured using unidirectional (UD) FlaxTape 200 preforms obtained from Ecotechnilin (France) with an areal weight of 200 g/m^2. The flax FRP laminates containing twisted fibres were manufactured using quasi-UD Amplitex 280 preform with an areal weight of 280 g/m^2, sourced from BComp (Switzerland). A quasi-UD glass preform with an areal weight of 1260 g/m^2 manufactured by Kush Synthetics (containing straight fibres) was chosen as benchmark for assessing the flax FRP composites fatigue performance. The same epoxy resin matrix system, SWANCOR 2511-1AL/BL, was chosen for all the laminates.

The laminate configuration selected are listed in Table 1. The first three lay-ups were selected to investigate the mechanical behaviour of predominantly UD flax fibres in which the behaviour is mainly fibre dominated. Although a fully unidirectional lay-up was initially considered, preliminary testing revealed a tendency for fatigue-induced splitting in such configurations. Consequently, 90° layers were incorporated to mitigate this splitting phenomenon. Additionally, a quasi-isotropic $[0/+45/-45/90]_S$ and an angle-ply laminate $[+45/-45]_{2S}$ were

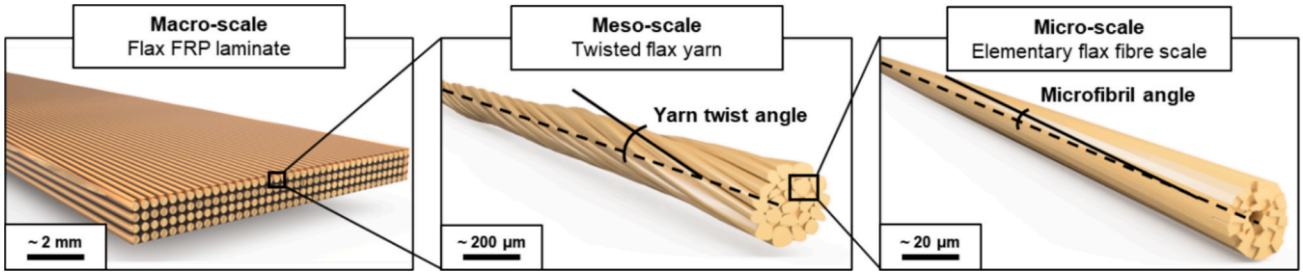

Fig. 1. Schematic 3D model of 3 levels of hierarchy in UD flax FRP laminates with yarn twist across different length scales at macro, meso, and micro levels.

Table 1
List of laminates used in the experimental campaign. The fibre volume fraction was calculated based on the specimen's geometry, weight, measured matrix density, and the average areal weight of the preform provided by the manufacturers.

Lay-up	Fibre type	Fibre orientation	Fabric model	Matrix	Thickness [mm]	Fibre volume fraction [%]
[0/90/0]	Glass	Straight	Kush SyntheticsHigh stiffness 1260	Epoxy resin system SWANCOR2511-1AL/BL	2.55 ± 0.02	58.3 ± 1.2
$[0/90/0]_S$	Flax	Straight	EcotechnilinFlaxtape 200		2.68 ± 0.10	32.1 ± 1.5
$[0/90/0]_S$	Flax	Twisted yarns	BcompAmplitex 280		2.87 ± 0.04	40.9 ± 1.1
$[0/+45/-45/90]_S$	Flax	Twisted yarns	BcompAmplitex 280		3.81 ± 0.03	42.4 ± 0.7
$[+45/-45]_{2S}$	Flax	Twisted yarns	BcompAmplitex 280		3.78 ± 0.09	43.4 ± 2.2

manufactured and tested to examine the evolution of laminate stiffness in cases where the mechanical response is not predominantly influenced by 0° plies (fibre dominated) but also matrix and interface dominated.

2.1.2. Manufacturing

Flax and glass FRP plates were fabricated using a vacuum-assisted resin infusion (VARI) process with the Swancor 2511–1 two component epoxy resin system. The fibres were infused under laboratory conditions (20 °C–22 °C and 30 %–50 % RH) without prior drying, as drying was observed to reduce the mechanical performance of flax FRP composites [22]. Following infusion, an 18-hour post-cure was conducted in an autoclave at 70 °C and 7 bars of pressure. To confirm complete resin curing, differential scanning calorimetry (DSC) analysis was performed post-manufacture with three heating/cooling cycles between 0 °C and 150 °C to ensure the glass transition temperature (Tg) differed by no more than 3 °C cycle to cycle. Optical microscopy was employed to qualitatively assess the microstructure of pristine specimens, verifying the absence of major cracks or manufacturing defects/voids and serving as a reference for microscopy post fatigue testing.

Coupon specimens used for mechanical testing were cut from the FRP plates using a waterjet cutter, with particular care taken to prevent moisture ingress. Throughout the cutting process, the specimens were maintained above the water level, thereby avoiding direct immersion. The cutting process lasted less than 20 min, and any water droplets deposited on the specimen surfaces were promptly wiped off upon completion. To assess whether the specimens remained near moisture equilibrium after cutting, a subset was placed in a climate chamber at 50 °C and 50 % relative humidity. This temperature was chosen to accelerate moisture diffusion while minimally affecting the equilibrium content. The observed weight change after 10 days ranged from + 0.18 % to − 0.12 %, indicating that the specimens were close to equilibrium with the testing humidity condition of 50 % RH.

Except for the rectangular geometry of the $[+45/-45]_{2S}$ specimens, the coupons were designed with a narrow central cross-section and wider cross-sections near the grips according to the plan in Fig. 2. This geometry was adopted to prevent failure at the clamp edges during fatigue testing, a problem observed in preliminary trials with rectangular coupons with or without end-tabs. Prior to testing, the coupon specimens were sanded in the tab region and high-density paper tabs were glued to increase friction in the clamps. The laminates tested are listed in Table 1.

2.2. Mechanical testing

2.2.1. Quasi-static tensile tests

To establish a reference for fatigue testing and to determine the ultimate tensile strength (UTS), five quasi-static tensile tests were conducted for each laminate. These tests were performed using an Instron 1251 hydraulic tensile testing machine, equipped with a Weisstechnik climate chamber maintained at a controlled temperature of 20 °C and a relative humidity (RH) of 50 %. The specimens were fitted with an extensometer to ensure accurate strain measurement and subjected to displacement-controlled tensile loading at a rate of 2 mm/min until failure.

To monitor and verify thermal conditions, two thermocouples were installed: one positioned on the surface of the specimen to confirm that the specimen reached the desired temperature, and the other placed in close proximity to the specimen to measure the air temperature within the chamber.

2.2.2. Fatigue tests without auxiliary loading sequences

To establish a reference for conventional fatigue testing, tension–tension fatigue tests were conducted on pristine specimens under a load ratio of R = 0.1, a frequency of f = 5 Hz, and a peak stress corresponding to 60 % of UTS determined from the quasi-static tensile tests. The specimens were equipped with an extensometer for precise strain measurement. Data were recorded for a complete loading–unloading cycle at a sampling rate of 250 Hz every 1′000 cycles to track the evolution of stiffness and the accumulation of deformation.

Due to laboratory constraints, two different machines were used for fatigue testing. Therefore, reference fatigue testing was first conducted on an Instron 1251 100 kN testing machine. This machine was equipped with a Weisstechnik climate chamber, as also used for the quasi-static tensile tests. Then the reference fatigue testing was repeated on a separate MTS 60 kN testing machine, which did not include a climate chamber, to account for any variability introduced by these different setups. In both setups, thermal probes were utilised to monitor the surface temperature of the specimens as well as the ambient air temperature in proximity to the specimen surface. The largest temperature elevation measured during fatigue on the surface of the specimens in the setup with climate chamber was 5 °C and 13 °C in the setup without the climate chamber, but in general the temperature elevation remained below 10 °C.

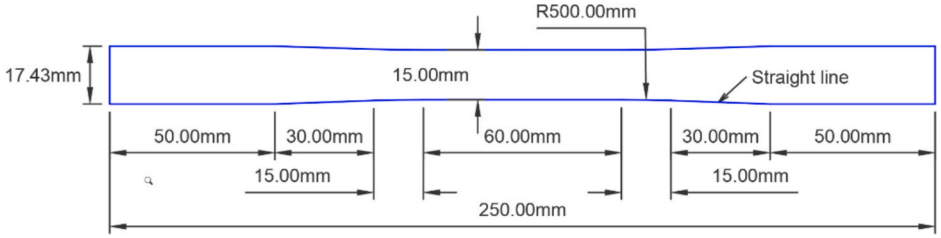

Fig. 2. Coupons specimens dogbone geometry. Chosen based on trials to minimize curvature while preventing tab failure.

2.2.3. Fatigue tests with pre-straining and pre-creeping

To examine the effects of preloading scenarios that might occur before structures enter into service, as exemplified by pre-creeping in the Ritsumasyl Bridge [6], two distinct preloading protocols were evaluated.

Pre-straining Protocol: Specimens were subjected to quasi-static loading at a displacement rate of 2 mm/min until reaching 80 % of the laminate ultimate tensile strength (UTS). At this load level, the specimens were immediately unloaded to zero load at the same displacement rate (2 mm/min). Subsequently, a conventional fatigue test was conducted, applying 60 % UTS with a stress ratio R = 0.1 and frequency f = 5 Hz. The details of this protocol are illustrated in Fig. 3 on the left.

Pre-creeping Protocol: Specimens were first subjected to a quasi-static displacement rate of 2 mm/min until 60 % of the laminate UTS was reached. This load level was maintained until a strain of 1.6 % was achieved for laminates with twisted flax fibres and 1.1 % for straight flax fibres. These strain levels were selected based on preliminary trial experiments to obtain equivalent creep durations of about 5 h across the two laminate configurations, thus providing a consistent basis for comparative analysis. specimens were then unloaded to zero load using the same displacement rate. Following this, a conventional fatigue test identical to the one described for the pre-straining protocol (60 % UTS, R = 0.1, f = 5 Hz) was performed. This protocol is illustrated in Fig. 3 on the right.

These testing protocols were conducted on the MTS 60 kN machine without climate control. As in previous tests, temperature was recorded using thermal probes and the strain was measured with an extensometer. During the pre-straining and pre-creeping phases, data was collected at a sampling rate of 2 Hz. For the fatigue phase, consistent with reference fatigue tests, data was recorded every 1′000 cycles for a complete loading–unloading cycle, with a sampling rate of 250 Hz.

2.2.4. Fatigue tests with loading interruptions

To investigate the effects of fatigue interruptions, a loading profile consisting of successive fatigue blocks of 10,000 cycles followed by 3-hour loading interruptions was applied to the laminates, as shown in Fig. 4. Due to technical constraints, the load level during interruptions was maintained between 3 % and 4 % of the UTS, rather than being completely unloaded. During the fatigue phase, data were recorded every 100 cycles for a complete loading–unloading cycle, using a sampling rate of 250 Hz. Additionally, continuous data recording at 1 Hz was conducted throughout the test to monitor strain during the loading interruptions.

The interrupted fatigue tests were performed using the Instron 1251 testing machine (100 kN capacity), with the climate chamber set to 20 °C and 50 % RH.

2.2.5. Characterisation of stiffness and strain

To characterise stiffness properties from quasi-static tests, the tangent modulus $E^{tan,1}$ was evaluated between the origin and 0.2 % strain as illustrated in Fig. 5 on the left. Because the tested flax FRP laminates exhibit a bilinear behaviour, a secondary tangent modulus, $E^{tan,2}$, was evaluated between 1 % and 1.5 % strain for those laminates.

In fatigue tests, the stiffness was defined as the secant modulus E_n^{sec} according to illustration in Fig. 5 on the right with the bottom index n corresponding to the cycle number. To quantify the stiffness evolution in fatigue the ratio of the secant modulus was taken as expressed by equation (1):

$$n_E = E_n^{sec} / E_1^{sec} \tag{1}$$

In fatigue, the strain was characterised at the bottom and top of the hysteresis as $\epsilon_{valley,n}$ and $\epsilon_{peaks,n}$ respectively. The strain accumulation was defined by equation (2):

$$\epsilon_n^{acc} = \epsilon_n^{peak} - \epsilon_1^{peak} \tag{2}$$

The ultimate strain in fatigue is expressed as ϵ_{peak,N_f} where N_f is the last loading cycle recorded before failure.

2.3. Microstructural visualisation

2.3.1. Micro-computed X-ray tomography

Micro-CT observations were performed on pristine specimens reinforced with straight and twisted fibres to qualitatively describe the difference in fibre arrangement. The measurements were performed on a TESCAN UniTOM HR. The scans were performed at 60 kV and 1.5 W with a voxel size of 1.5 µm without binning. Over the 360° rotation of the sample, 3500 projections were acquired, each with an exposure time of 380 ms and an averaging over 7 frames to reduce random noise. The total acquisition time was 226 min. The visualization images were obtained with the Avizo software.

2.3.2. Optical microscopy

To observe the damage morphologies within the microstructure of flax FRP laminates, samples with dimensions of 15 mm (length) × 15 mm (width) were cut post-mortem from specimens subjected to fatigue loading using a wood bandsaw. Samples were also extracted from post-

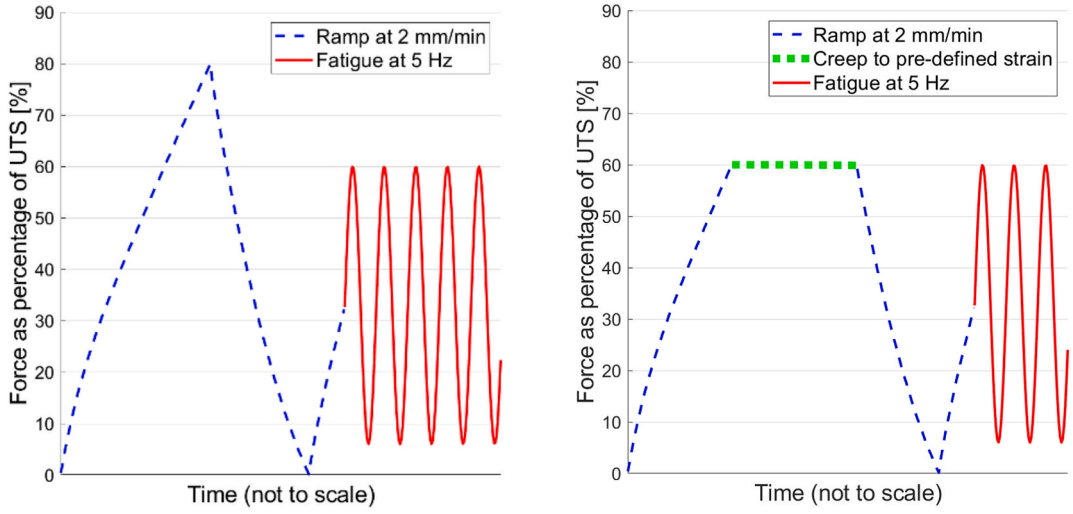

Fig. 3. Loading profile of pre-straining (left) and pre-creeping (right) followed by continuous fatigue.

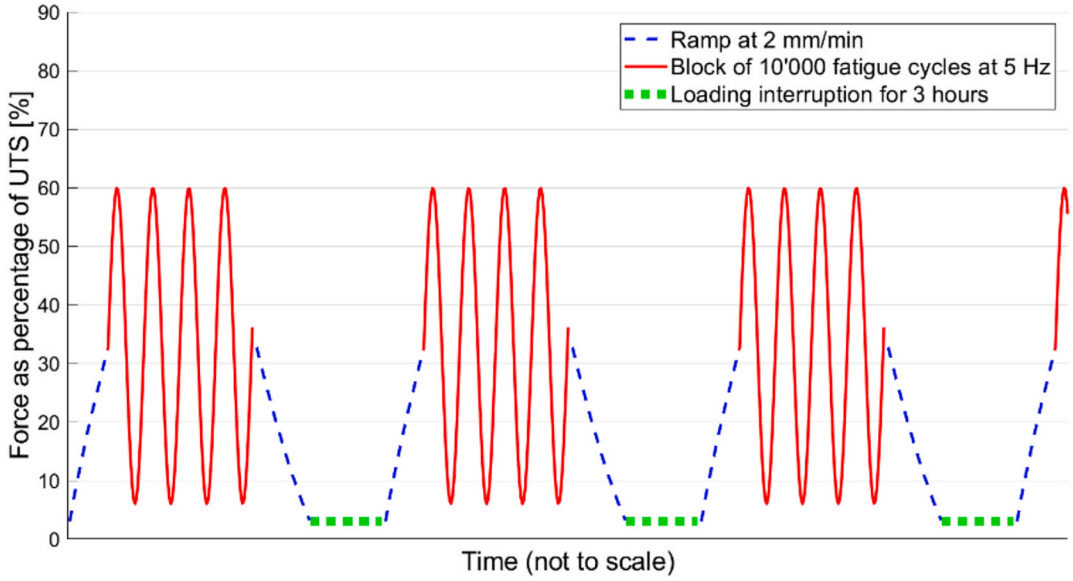

Fig. 4. Loading profile of interrupted fatigue.

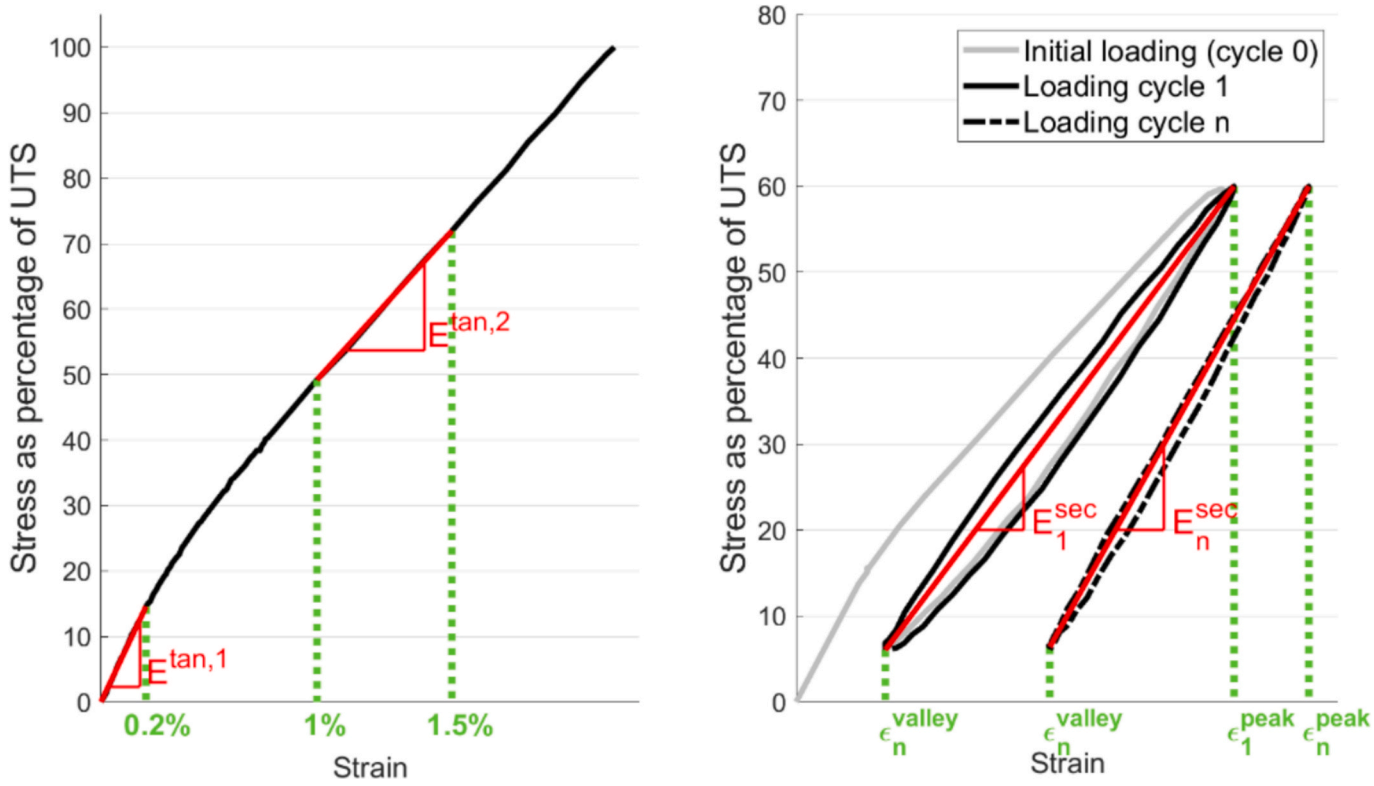

Fig. 5. Definition of the tangent modulus from quasi-static tests (left), and the secant modulus from fatigue tests as well as peak and valley strains (right).

mortem glass FRP laminates with a diamond saw. The samples were then embedded in Struers EpoFix resin. The embedded specimens were grinded and polished using a Struers Tegramin-20 polishing machine, adhering to the "Epoxy – Soft and ductile" protocol provided by Struers for the flax FRP specimens. The glass FRP specimens were polished following the Struers "Fibers – Fragile fibers" protocol. Microstructural imaging was then conducted on the polished samples using a Keyence VK-X1000 confocal scanning microscope.

3. Results and discussion

3.1. Variability in material and in quasi-static performance

Quasi-static tensile tests were performed to determine the ultimate tensile strength (UTS) of the laminates and to define the corresponding stress levels for subsequent fatigue testing. These tests were conducted on straight glass fibre laminates [0/90/0] straight flax fibre laminates $[0/90/0]_S$ and twisted flax yarn laminates $[0/90/0]_S$, as summarised in Table 2. The results revealed a notably higher standard deviation in UTS

Table 2
Strength and modulus results obtained from quasi-static tensile tests demonstrating the specimen-to-specimen variability in mechanical properties. The means and standard deviations are indicated in bold.

	UTS [MPa]					
	Sample					mean ± stdv
	1	2	3	4	5	
Straight glass fibres	526	615	627	711	735	643 ± 83
Straight flax fibres	174	185	199	208	217	197 ± 18
Twisted flax yarns	222	223	223	228	229	225 ± 4

	$E^{tan,1}$ [GPa]						$E^{tan,2}$ [GPa]					
	Sample					mean ± stdv	Sample					mean ± stdv
	1	**2**	**3**	**4**	5		1	2	3	4	5	
Straight glass fibres	39.7	38.5	38.8	39.8	38.1	39.0 ± 0.7	–	–	–	–	–	–
Straight flax fibres	14.7	16.3	17.2	17.4	17.6	16.6 ± 1.2	10.2	11.0	12.2	12.5	12.8	11.7 ± 1.1
Twisted flax yarns	17.4	17.1	16.3	16.2	17.9	17.0 ± 0.7	8.8	9.4	8.6	8.7	9.4	9.0 ± 0.4

for the straight flax fibre laminates (18 MPa) compared to the twisted flax yarn laminates (4 MPa). The greater variability is attributed to the pronounced inhomogeneity in the straight flax fibre preform, which leads to a higher degree of fibre volume fraction variability across the manufactured plate and hence between specimens. This is visually apparent under transmitted light inspection, as illustrated in Fig. 6. Furthermore, straight flax fibre preform is fragile and difficult to handle without inducing fibre misalignment or damage, limiting repeatability and precision.

This hypothesis is supported by a correlation between UTS and tensile modulus within the straight flax fibre laminates: higher UTS values were associated with higher stiffness, which can be explained by higher fibre volume fraction. However, for the straight glass fibre laminate and twisted flax yarn laminates, the UTS and tensile modulus are not correlated, suggesting that their scatter is not directly related to variations in fibre volume fraction.

The standard deviation in the UTS of the glass fibre laminates, 83 MPa, was found larger than in the twisted flax yarn laminates, 4 MPa, even when normalised by the average UTS. This can be attributed to the brittle failure mode of the glass fibre laminate (see Fig. 7), which limits stress redistribution upon local failure. As a result, the mechanical

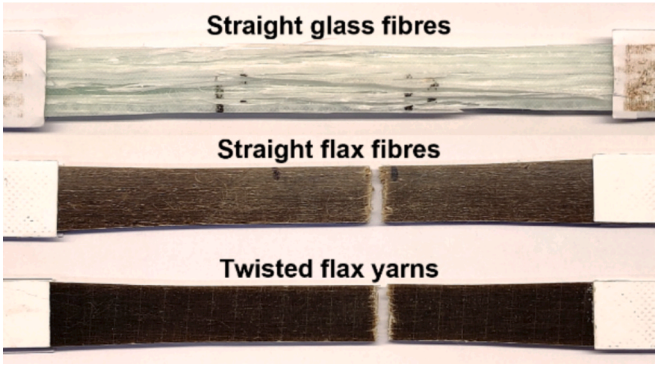

Fig. 7. Comparison of quasi-static tensile failure showing localised failure in flax FRP laminates and brittle failure over the entire specimen surface in the glass FRP laminate.

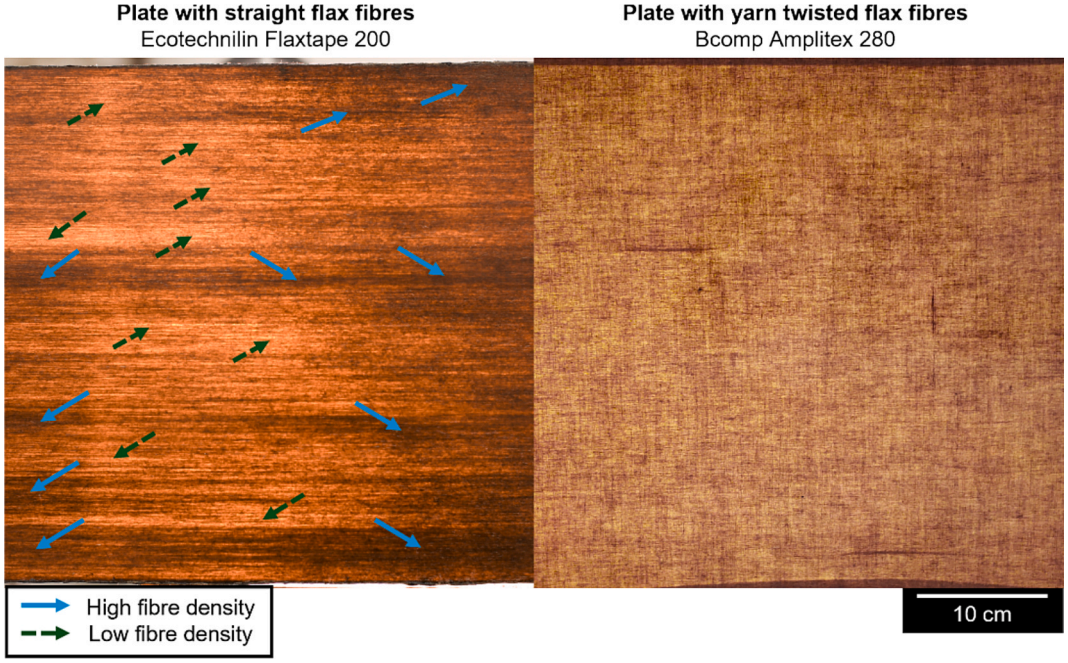

Fig. 6. Illustration of fibre inhomogeneity in laminate with straight fibres (left) compared to fibre homogeneity in laminate with twisted yarn (right) by shining light through the plate. Both laminates were manufactured with the same resin and following the same manufacturing protocol.

performance of the glass laminates is more sensitive to local imperfections than in laminates reinforced by flax fibres introducing plasticity.

To provide a 3-dimensionnal visualisation of the difference in fibre architecture between a straight flax fibres laminate and twisted flax yarns laminate, micro-CT scans of corresponding unidirectional laminates are shown in Fig. 8.

3.2. Influence of preloading and load interruptions on fatigue performance

Strain accumulation, stiffness evolution, and fatigue life were investigated under various load sequences, including pre-straining, pre-creeping, and fatigue interruptions. The influence on fatigue performance was assessed in relation to both the intrinsic properties of the fibres by comparing the straight glass fibres laminate with the straight flax fibres laminate, and their fibre/yarn microstructural arrangements by comparing the straight flax fibre laminate with the twisted flax yarns laminate.

3.2.1. Stiffness evolution and strain accumulation in continuous fatigue

To serve as a baseline for fatigue under standard testing conditions on pristine specimens subjected to continuous fatigue, Figs. 9 and 11 show fatigue results for straight glass fibres and straight flax fibres/twisted flax yarns, respectively. In those graphs, the evolution of E_n^{sec}/E_1^{sec} and strain accumulation $\epsilon_n^{peak} - \epsilon_1^{peak}$, (according to the definition in Fig. 5), are plotted against the normalised fatigue life n/N_f. Additionally, optical microscopy images illustrating the post-fatigue cracking patterns within the 90° plies for each laminate configuration are presented in Figs. 10, 12, and 13.

In the straight glass fibres laminate, the evolution of E_n/E_1 was observed to follow the typically expected stiffness degradation consisting of an initial quick reduction in stiffness, followed by a slower and more stable decrease of the modulus for the larger part of the fatigue cycles, with finally a sharp modulus decrease leading to failure [23–25]. Since the test depicted in Fig. 9 was a tension–tension fatigue test exhibiting brittle failure following a brief reduction in modulus, the decline in modulus immediately preceding failure was not recorded. This was due to the limitation of hysteresis data acquisition, which was conducted at intervals of every 1,000 loading cycles. The observed stiffness degradation can be correlated to the development of cracks illustrated in Fig. 10. These cracks follow the surface of fibres in fibre-rich region and continue in the matrix-rich regions. They often span the full or nearly full thickness of the 90° plies and terminate at the interface with the 0° plies. As these transverse cracks grow under fatigue loading, they are expected to reduce the effective cross-sectional area of the laminate, leading to a progressive reduction in its effective stiffness.

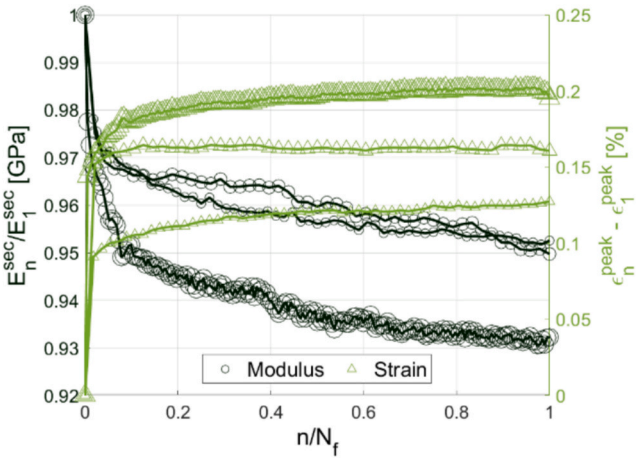

Fig. 9. Evolution of strain accumulation and modulus decrease in fatigue of glass FRP. The three repetitions for each test are distinguished with different marker sizes.

In the straight flax fibre laminate, the modulus was observed to increase sharply at the beginning of fatigue life, with a maximal stiffness increase of approximately 10 % reached at 20 % of the fatigue life. While an increase in stiffness during fatigue is peculiar for synthetic FRP composites, it is a known phenomenon for flax FRP composites intrinsic to flax fibres as cyclic tests on both flax composites and single flax fibres have demonstrated an increase in modulus under tension–tension fatigue loading [26–29]. Yet, as seen in Fig. 11 on the left, E_n^{sec}/E_1^{sec} is decreasing after 20 % of fatigue life suggesting that competing mechanisms are at play in the laminate. The fibre stiffening is progressively outweighed by the accumulation of damage within the composite. This damage is visible in Fig. 12, where cracking patterns similar to those observed in glass fibre laminates are identified. These cracks follow the fibre surface and propagate through matrix-rich regions, and in some areas, traverse entirely across the 90° plies. As with glass FRP laminates, such cracking is expected to reduce the effective load-bearing cross-section, thereby contributing to stiffness degradation during fatigue.

In the twisted flax yarn laminate, no stiffness degradation was observed during fatigue (Fig. 11 on the right). This absence of stiffness degradation can be partially attributed to the distinct cracking pattern associated with twisted yarns, illustrated in Fig. 13. In contrast to laminates reinforced with straight fibres, twisted flax yarns exhibit a cracking pattern where cracks are predominantly confined within the

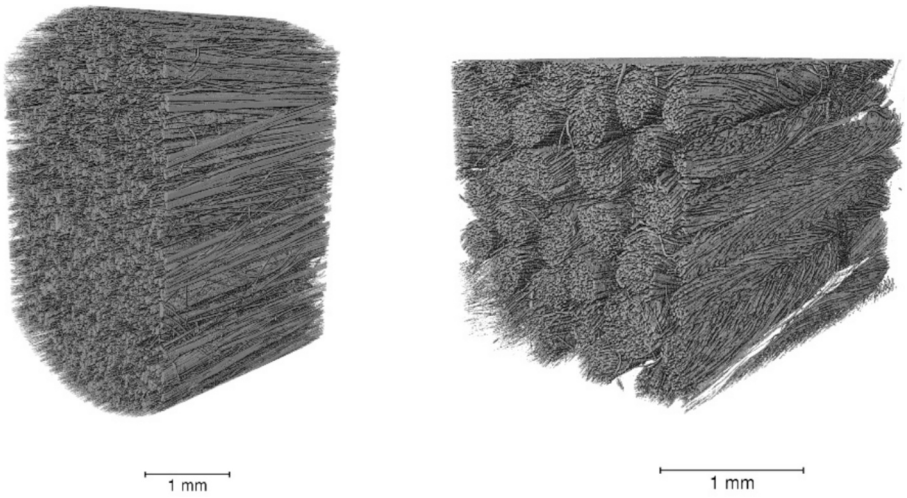

Fig. 8. Micro-CT scans of flax FRP specimen comparing fibre arrangement with straight fibres (left) and twisted yarns (right).

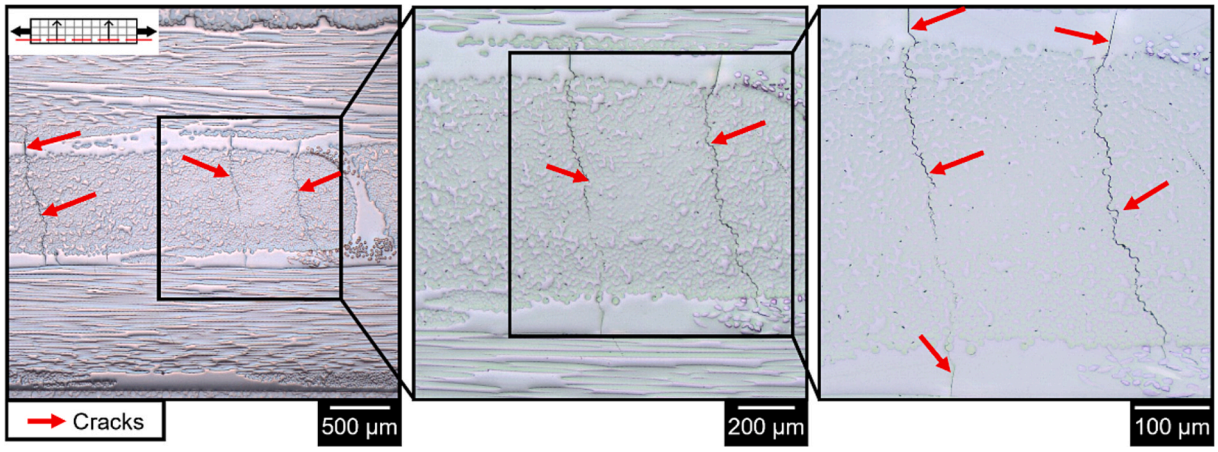

Fig. 10. Optical microscopy of glass FRP laminates reinforced with straight glass fibres. Crack at the fibre–matrix interface and through the matrix after fatigue testing are indicated with arrows. This fatigue test was stopped before final failure to maintain the structure of the specimen for microscopy.

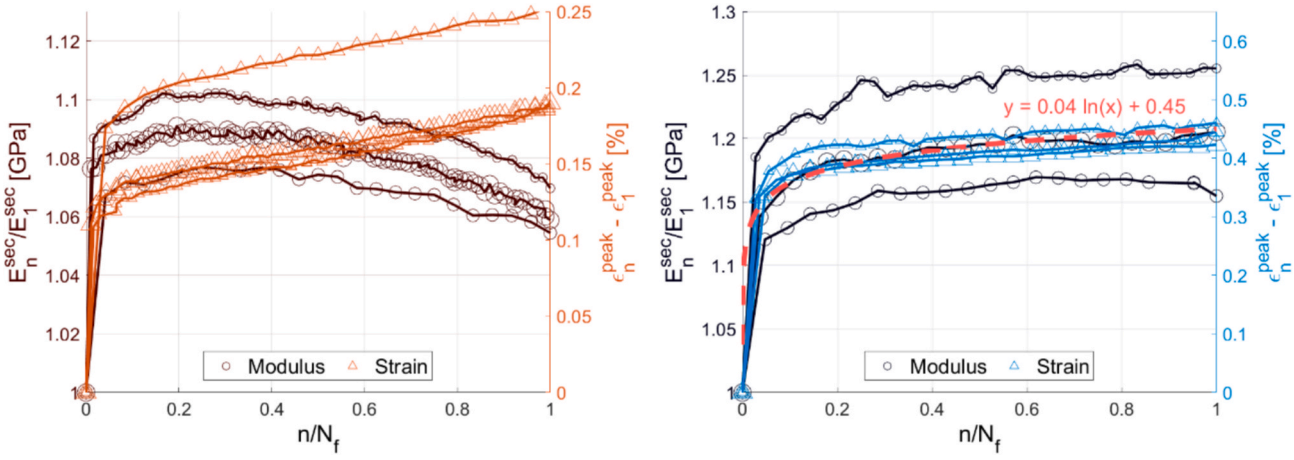

Fig. 11. Evolution of strain accumulation and modulus increase in flax FRP reinforced with straight fibres (left). Proportional evolution of strain accumulation and modulus increase in flax FRP reinforced with twisted fibres (right). The strain is approximated with a logarithmic trend.

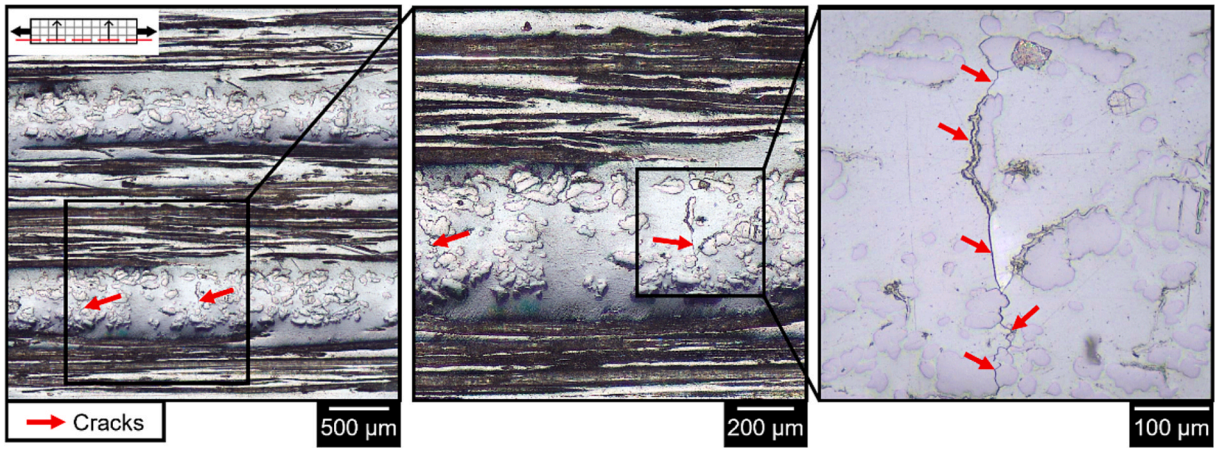

Fig. 12. Optical microscopy of FRP laminates reinforced with straight flax fibres after fatigue testing. Cracks at the fibre–matrix interface and through matrix cracks are indicated with arrows.

yarns, while matrix-rich regions largely remain uncracked. Although the presence of cracks within the yarns is expected to reduce the effective cross-sectional area of the 90° plies and thus contribute to stiffness degradation, the extent of this reduction appears to be less severe than in laminates with straight fibres. Furthermore, the measured E_n^{sec}/E_1^{sec} increase is approximately twice larger with twisted flax yarns than with straight flax fibres, suggesting that the helical structure introduced by the yarns plays a crucial role on the modulus evolution in fatigue. It is hypothesised that re-arrangement of flax fibres within the helical structure of the yarn induces contributes to this larger stiffening. This

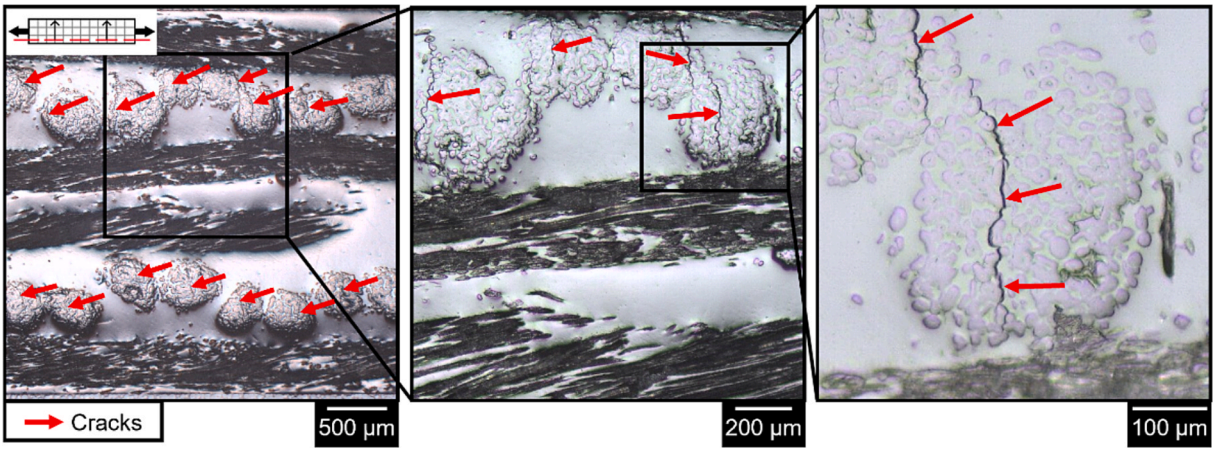

Fig. 13. Optical microscopy of FRP laminates reinforced with twisted flax fibres after fatigue testing showing intra-yarn cracks indicated with arrows and no through matrix cracks.

effect of yarn untwisting on the stiffness increase will be further scrutinised in section 3.2.2.

Regarding strain accumulation in fatigue, laminates with straight fibres experienced a strain accumulation of approximately 0.2 % over their entire fatigue life while twisted flax yarns laminate accumulated 0.4 % strain. This doubling in strain accumulation suggests that re-arrangement occurs not only at the micro-scale with microfibrils alignment [18,30,31] but also at the *meso*-scale with a reduction of the yarn twist angle.

The above observation of stiffening effect during fatigue was made for a fibre-dominated laminate lay-up configuration, $[0/90/0]_S$, where the load is aligned with fibre or yarn axis. To evaluate the effect of lay-up on the stiffening mechanism, an angle-ply $[+45/\text{-}45]_{2S}$ and a quasi-isotropic $[0/+45/\text{-}45/90]_S$ laminate manufactured with the twisted yarn preform were tested and compared with their $[0/90/0]_S$ counterpart. Fig. 14 shows that the lay-up configuration plays a key role in the evolution of stiffness in fatigue. The angle-ply laminate exhibits a stiffness decrease over the entire fatigue life in contrast with the fibre-dominated laminates. This demonstrates that the stiffening mechanisms are majorly absent in the angle ply laminates due to the off-fibre axis loading while numerous interface cracks or matrix might occur. Coincidentally, E_n^{sec}/E_1^{sec} remained constant during fatigue suggesting a balance between stiffening mechanism in the 0° plies and crack initiation and propagation in the 45° and 90° reducing the effective stress transfer, thus reducing stiffness.

3.2.2. *Pre-straining and pre-creeping effects enhancing fatigue performance*

The increase in modulus observed under continuous fatigue was observed to correlate with strain accumulation for flax FRP laminates particularly remarkable in the case of twisted flax yarns reinforcement (Fig. 11 on the right). Therefore, pre-straining (short term loading) and pre-creeping, (long-term loading) were applied to specimens prior to fatigue loading to induce micro-structural re-arrangement beneficial for fatigue performance. Fig. 15, Fig. 16, and Fig. 17, each for a different laminate compare the fatigue modulus, E_n^{sec}, and strain accumulation, $\epsilon_n^{peak} - \epsilon_1^{peak}$ of pristine, pre-strained, and pre-creeped specimens.

The average modulus in straight glass fibre laminates shown in Fig. 15 increased with pre-creeping by 4 % relative to the average modulus of pristine specimens. Further alignment of polymeric chains of the matrix or glass fibres during creep could contribute to this modulus increase. No reduction of strain accumulation in fatigue was observed after pre-straining nor after pre-creeping for this laminate.

The results of the straight flax fibre laminate presented in Fig. 16 exhibit a large scatter related to the inhomogeneity of the preform

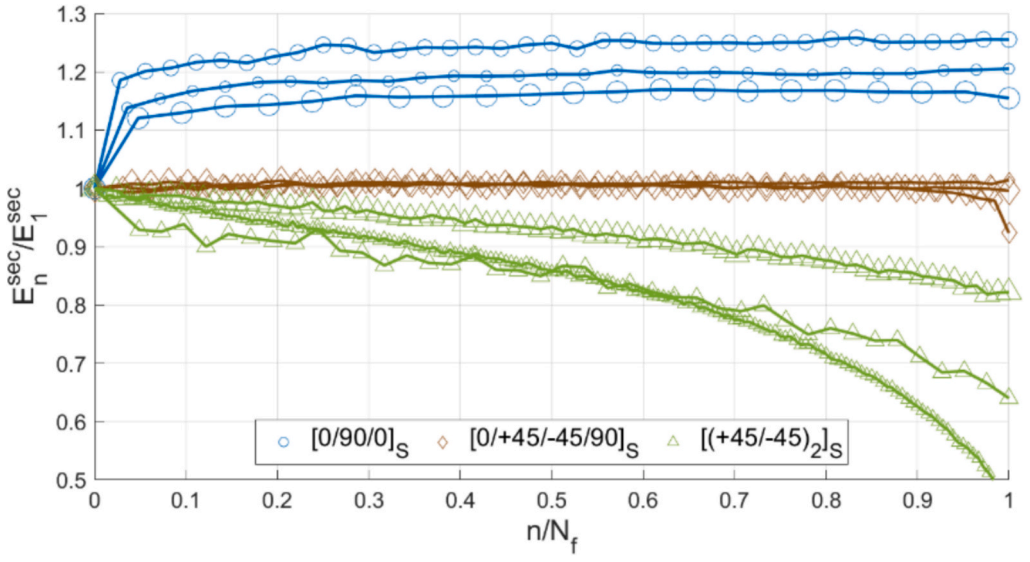

Fig. 14. Stiffness evolution in fatigue for twisted flax FRP laminates with different lay-ups. The three repetitions for each test are distinguished with different marker sizes.

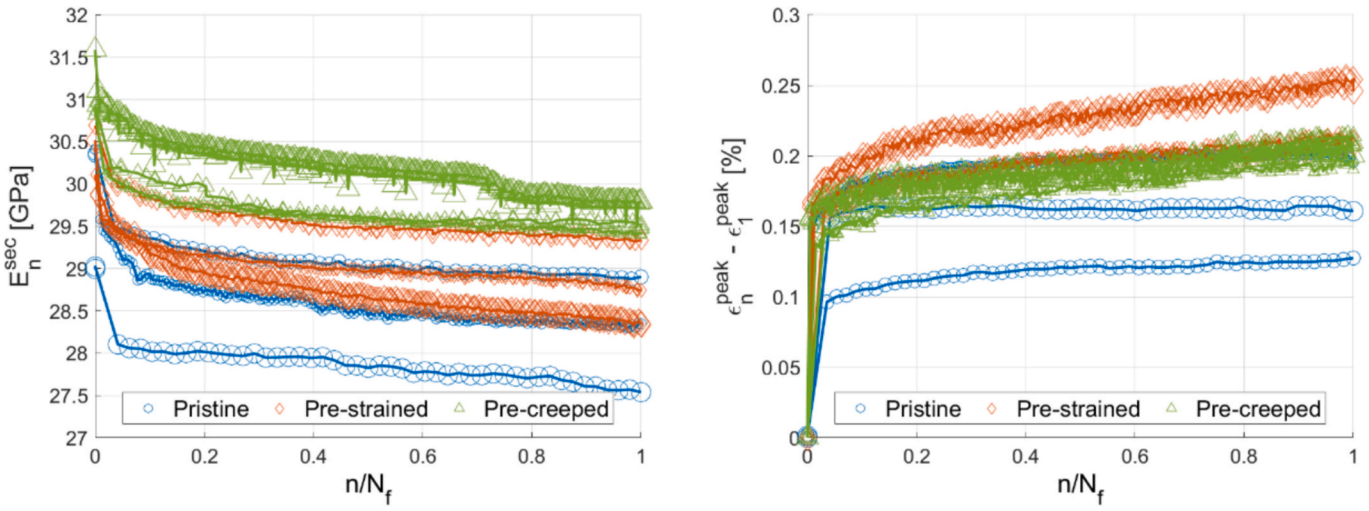

Fig. 15. Evolution of modulus (left) and strain accumulation (right) for glass FRPs with straight fibres during fatigue loading with different types of preloading. The three repetitions for each test are distinguished with different marker sizes.

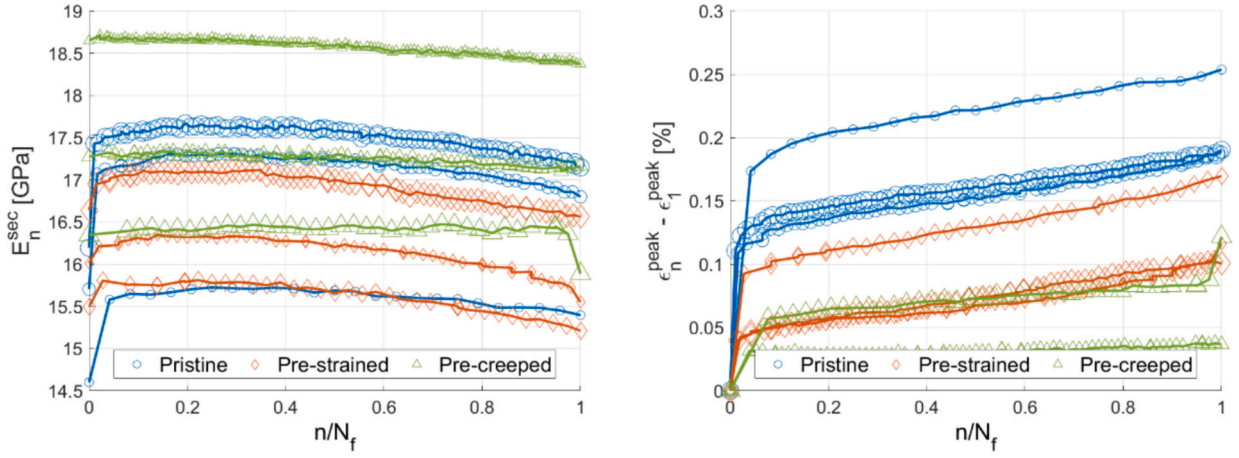

Fig. 16. Evolution of modulus (left) and strain accumulation (right) of flax FRPs with straight fibre during fatigue loading with different types of preloading. The three repetitions for each case are distinguished with different marker sizes.

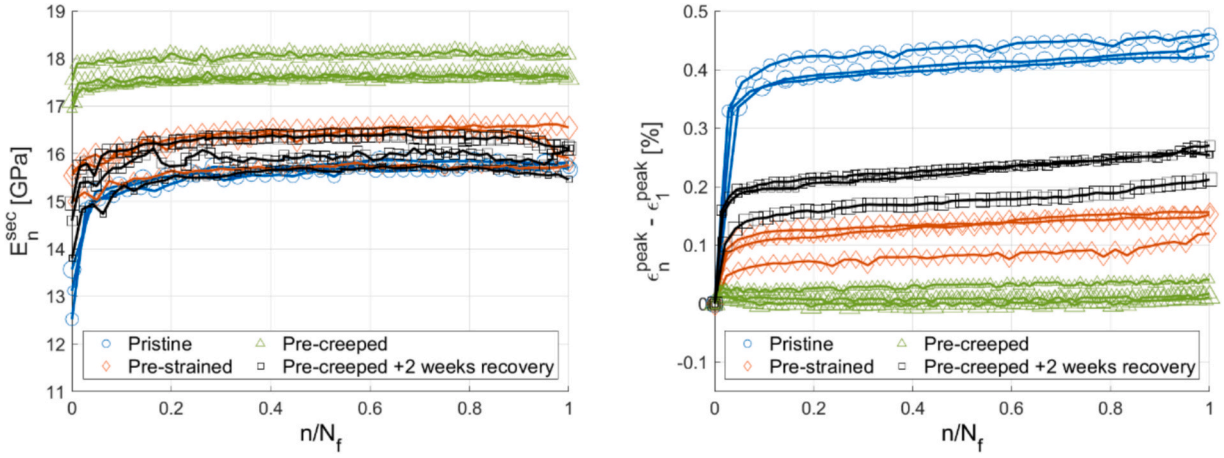

Fig. 17. Evolution of modulus (left) and strain accumulation (right) of flax FRPs with twisted fibres during fatigue with different types of preloading. The three runs for each case are distinguished with different marker sizes.

illustrated in Fig. 6. Yet, clear effects of pre-straining and pre-creeping can be observed with an increase in modulus and reduction of strain accumulation. Interestingly, during fatigue of pre-creeped specimens, E_n is only decreasing but starts on average 12 % higher than in pristine specimens. This suggests that the re-arrangement normally occurring in fatigue already took place during pre-creeping. Furthermore, re-arrangement during pre-creeping in place of during fatigue is supported by the reduction of strain accumulation $\epsilon_n^{peak} - \epsilon_1^{peak}$.

The laminates reinforced with twisted flax yarns exhibited trends similar to those observed in straight flax fibre laminates, albeit with reduced data scatter and increased effect magnitudes (Fig. 17). With twisted flax yarns, the average secant modulus on the first fatigue loading cycle, E_1^{sec}, was measured 32 % higher on pre-creeped specimens than on pristine specimen. Additionally, pre-creeped specimens exhibited negligible strain accumulation relative to the strain accumulation of pristine specimens. In comparison, pre-creeping specimens with straight flax fibre resulted in a 12 % larger E_1^{sec} than in pristine specimens and halved the strain accumulation. Given the substantial benefits of pre-creeping yet recognising the viscoelastic nature of flax fibres and the potential reversibility of such effects over time, an additional recovery test was implemented. This involved a two-week rest period between pre-creeping and fatigue testing, during which the specimen was removed from the tensile testing setup. The results indicated that the improvements in stiffness and reduction in strain accumulation due to pre-creeping were partially reversed following recovery, aligning more closely with the effects observed from pre-straining.

The effects of pre-straining and pre-creeping on fatigue life are detailed in Table 3 with indication of the average and standard deviation. For straight glass fibres laminates and straight flax fibre laminates, the standard deviation is too large relative to the average to conclude a statistically significant effect. However, the twisted flax yarn laminate exhibited a small scatter allowing for the identification of a statistically significant effect on fatigue life with a 1.4-fold increase with pre-straining and 3-fold increase after pre-creeping. With pre-creeping and recovery, a significant increase in fatigue life is also observed relative to pristine specimens with a 2-fold increase. The remarkably consistent fatigue life obtained with the twisted flax yarns laminate is in accordance with the consistency observed in the UTS obtained in the quasi-static tests (Table 2).

The ultimate strain measured in fatigue, $\epsilon_{N_f}^{peak}$ as defined in Fig. 5, was observed to be negligibly influenced by pre-creeping across the three tested flax FRP laminates (Table 3). In contrast, pre-straining led to a slight increase in ultimate strain, particularly evident in the laminate containing twisted yarns. This increase suggests that the pre-straining load of 0.8 UTS, which is higher than the 0.6 UTS used during pre-creeping, induces a degree of permanent deformation not observed under the lower loading condition, even in the presence of time-dependent effects such as creep.

Regarding the efficacy of preloading specimens for increasing fatigue performance it was found that pre-creeping is particularly effective with a 3-fold increase in fatigue life. This can be explained by the increase in stiffness reducing the strain amplitude every cycle, thereby slowing the rate of damage growth. Yet, it remains to be explained how the modulus of the twisted flax laminate can be increased by a surprising 32 % while the increase of 12 % in the straight flax laminate should already capture the effects related to the intrinsic properties of flax fibres such as MFA alignment [18] and crystallisation [32]. For this we turn to the helical structure introduced with the yarn twist.

The yarn twist angle θ was estimated based on optical microscopy of the flax yarns (Fig. 19 on the left). This angle was determined to be a mean of 16.2° over 18 measures with a standard deviation of 1.6° which is in the range found in literature of 5° to 25° [20,33,34]. Calculations were done with $\theta = 16°$. Based on the assumption of θ on a cylinder with a constant volume and a longitudinal strain accumulation of 0.7 % as measured after pre-creeping, the calculation yields a new yarn twist angle of 15.84°. To estimate the contribution of this 0.16° fibre alignment (untwisting) on the composite we used the simplest model relating stiffness and the fibre angle [35]:

$$E_{eff} = E\cos^2\theta \tag{3}$$

with E a constant corresponding to the assumed stiffness of the untwisted yarn. Solely based on a change of fibre angle θ from 16° to 15.84° with pre-creeping, this calculation results in a 0.16 % increase in E_{eff}, orders of magnitude below the 32 % increase measured experimentally. Therefore, the simple alignment of fibres cannot explain the modulus increase. However, considering the helical structure of the yarn, a small yarn twist angle reduction can lead to a significant modulus increase considering resistance to volume change in the helix. Hearle [35] listed equations showing contribution to modulus in deformation of helical structures including the equation for volume change:

$$E_{eff} = K(1 - 2\cot^2\theta)^2 \tag{4}$$

with K being material properties. Computing again the effective modulus variation with a θ angle change from 16° to 15.84°, assuming K constant, suggests a 4.5 % increase in modulus. To this, the 12 % stiffening measured in the straight flax fibre laminate should be added to account for stiffening of the elementary flax fibres at the micro-scale. This yields, with multiple assumptions, an estimated 16.5 % increase in E_{eff}. This value is still below the measured stiffness increase but demonstrates that the preform helical structure can play a significant role in the stiffness of the composite. The remaining discrepancy may be due to additional mechanisms induced by sustained loading in the twisted yarn composites. These may include internal stress relaxation

Table 3
Results of pre-straining and pre-creeping effects on fatigue life and ultimate strain.

		Fatigue life [k]				Ultimate strain [%]			
		Sample			mean ± stdv	Sample			mean ± stdv
		1	2	3		1	2	3	
Straight glass fibres	**Pristine**	48	56	192	**99 ± 81**	1.20	1.20	1.23	**1.21 ± 0.02**
	Pre-strained	97	149	236	**161 ± 70**	1.19	1.25	1.25	**1.23 ± 0.04**
	Pre-creeped	64	126	397	**196 ± 177**	1.28	1.23	1.16	**1.22 ± 0.06**
Straight flax fibres	**Pristine**	24	62	93	**60 ± 34**	1.08	0.96	0.94	**0.99 ± 0.08**
	Pre-strained	36	50	73	**53 ± 18**	1.15	1.05	0.96	**1.05 ± 0.10**
	Pre-creeped	40	77	136	**84 ± 49**	1.14	1.04	0.75	**0.98 ± 0.20**
Twisted flax yarns	**Pristine**	21	29	37	**29 ± 8**	1.46	1.44	1.56	**1.49 ± 0.06**
	Pre-strained	41	42	42	**42 ± 1**	1.67	1.56	1.56	**1.60 ± 0.06**
	Pre-creeped	77	89	97	**88 ± 10**	1.52	1.54	1.53	**1.53 ± 0.01**
	Pre-creeped and recovery	61	67	49	**59 ± 9**	1.19	1.18	1.27	**1.21 ± 0.05**

Note: The ultimate strain indicated for 'Pre-creeped and recovery' does not account for permanent strains accumulated during the pre-creeping phase and recovery.

within the helical structure, enhanced fibre–fibre friction in the yarns due to compaction, and local matrix flow or rearrangement in the resin rich areas around the yarns. Such effects are likely negligible in straight fibre composites, which lack the structural complexity of twisted yarns.

As the reduction of the yarn twist angle, θ, was evaluated with a geometrical model in the calculation above based on the total specimen geometry, an experiment was devised to make a direct measurement of the change of the angle θ. A specimen was first subjected to a micro-CT scan, then subjected to pre-creeping, and final subjected to a micro-CT scan again at the same location. 2D plans were then extracted from the 3D scan, indicated by L1 to L4 in Fig. 18, and the angle of the fibres in specific locations were measured visually as shown in Fig. 19. The measurements of angle in L1 gives an average θ reduction of 0.1° with pre-creeping, however this measurement method is not accurate with, in this case, a standard deviation of 0.7°. Nevertheless, these measurements confirm that the variation in yarn twist angle due to pre-creeping is minimal, remaining below 1°.

The stiffening induced by the yarn twist angle reduction at the *meso*-scale is analogous, albeit at a larger scale, to the alignment of microfibrils within elementary flax fibres, which has been directly observed using synchrotron X-ray diffraction [18,31]. Several researchers have cited this microfibrillar angle alignment to explain the stiffening observed in fatigue of flax FRP composites [28,29,36–40]. However, to the authors' knowledge, the yarn twist angle alignment presented in this paper has not been previously identified as a factor in explaining fatigue-induced stiffening, and thereby this phenomenon is elaborated here.

The results presented above demonstrate that pre-creeping is an effective strategy for enhancing the fatigue performance of flax fibre-reinforced polymer composites. This effect is most evident in laminates reinforced with twisted flax yarns, where pre-creeping led to a substantial 32 % increase in initial modulus and a three-fold extension of fatigue life, accompanied by near elimination of strain accumulation. These improvements are attributed to a combination of microstructural re-arrangements occurring at multiple scales: alignment of microfibrils within the elementary flax fibres at the micro-scale, and reconfiguration of the helical yarn architecture at the *meso*-scale. In contrast, the more modest enhancements observed following pre-straining are likely limited to microfibrillar alignment, as the absence of a helical structure in straight fibre configurations does not allow for significant *meso*-scale re-arrangement effects. Similar improvements in stiffness and fatigue performance following pre-straining or pre-creeping have been previously observed in natural fibre composites [21,41] but without investigation of the underlying multi-scale mechanisms. Furthermore, the observed reduction in strain accumulation with pre-creeping supports its applicability in structural contexts, as demonstrated in the Ritsumasyl Bridge, where pre-loading of flax FRP components was employed to reduce long-term deformations[6].

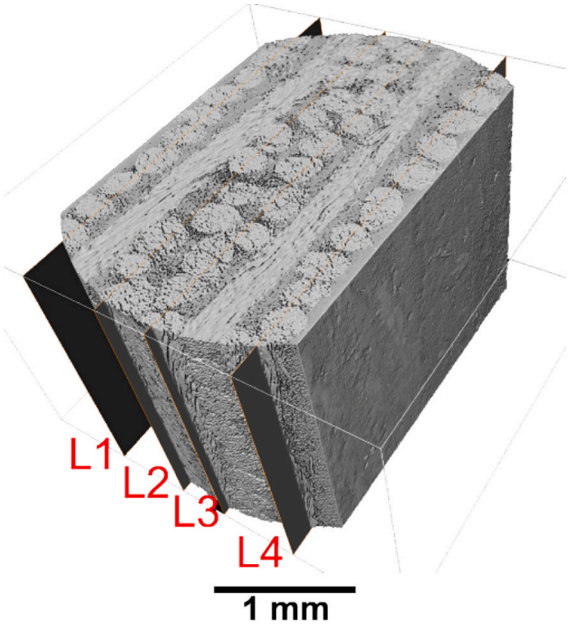

Fig. 18. 3D view of the flax FRP laminate with twisted yarn using Micro-CT scan with the indication of 4 cutting planes L1 to L4 in the 0° plies.

3.2.3. *Effect of loading interruptions on fatigue response*

In realistic structural applications, fatigue loading is often subjected to interruptions. To assess the relevance of such effects, interrupted fatigue tests were conducted on predominantly UD flax and glass FRP laminates. For the laminate reinforced with glass fibres, which exhibit predominantly elastic behaviour, interruptions were hypothesised to have negligible impact on fatigue performance. By contrast the laminates reinforced with viscoelastic flax fibres were expected to show a measurable response to loading interruptions. This was verified experimentally, and results are subsequently demonstrated in Fig. 20 and Table 4. Fig. 20 shows the evolution of dynamic stiffness during interrupted fatigue which highlights a clear difference between laminates reinforced with glass fibres, and laminates reinforced with flax fibres. The [0/90/0] straight glass fibres laminate, representing the elastic case, showed a nearly identical reduction in stiffness during interrupted fatigue compared to continuous fatigue, despite the implementation of 3-hour interruptions every 10′000 cycles. This consistent stiffness degradation pattern suggests that the stiffness loss is primarily governed by damage accumulation, which appears unaffected by the imposed unloading and subsequent recovery periods. In contrast, both viscoelastic flax FRP laminates exhibited stiffness increases during blocks of fatigue loading, as observed in continuous fatigue. However, a stiffness drop of up to 6.8 % was observed between the final loading cycle prior to interruption and the first cycle following resumption.

With reference to the strain accumulation illustrated in Fig. 20, the straight glass fibre laminate exhibits negligible sensitivity to fatigue interruptions. The observed strain recovery during the 3-hour loading pause is limited to approximately 0.01 %, and this minor recovery is immediately reversed upon resumption of fatigue loading. In contrast, the straight flax fibre laminate and the twisted flax yarn laminate display more pronounced strain recovery, each reaching approximately 0.05 % during the same interruption period. Following the recommencement of cyclic loading, strain continues to accumulate progressively, accompanied by an increase in stiffness. This observed correlation between strain and modulus evolution aligns with the behaviour identified under uninterrupted fatigue loading, as depicted in Fig. 11.

For the three laminates tested in continuous and interrupted fatigue, comparison of the fatigue life and ultimate strain are presented in Table 4. For the straight glass fibre and straight flax fibres, results suggest that fatigue interruptions do not have a significant impact on fatigue life nor on ultimate strain. However, results of the twisted flax yarns laminate show a statistically significant difference, indicating an increase of fatigue life with loading interruptions and an increase of ultimate strain.

The observed extension in fatigue life for the laminates reinforced with twisted flax yarns under interrupted loading conditions is hypothesised to be linked to the strain recovery. The measured strain recovery during interruptions (driven by the viscoelasticity of twisted flax yarns and the matrix) is hypothesized to partially close cracks (particularly intra-yarn cracks as shown in Fig. 13) induced during fatigue blocks. During cyclic loading, cracks progressively open as damage accumulates. However, it is hypothesised that upon interruption of loading, strain recovery, driven by the viscoelastic response and the unloading itself, may induce partial crack closure. When fatigue loading is resumed, these cracks re-open, but for a limited number of cycles, highlighted by the pink lines in Fig. 20, it is hypothesised that no further propagation occurs. Instead, the laminate may undergo re-opening of

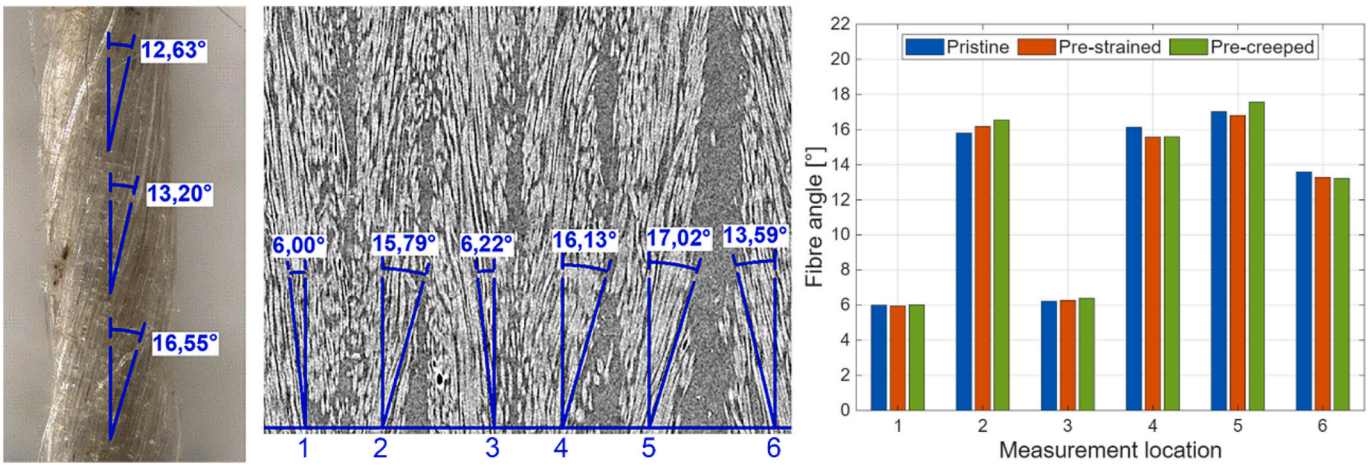

Fig. 19. Measurement of yarn twist angle on optical microscopy image of flax yarn extracted from Bcomp Amplitex 280 preform (left) and fibre angle measurement on micro-CT scan of pristine flax FRP specimen (middle). The bar plot (right) compares the fibres angle for the same specimen in the pristine state, after pre-straining, and after pre-creeping based on micro-CT scan after each step.

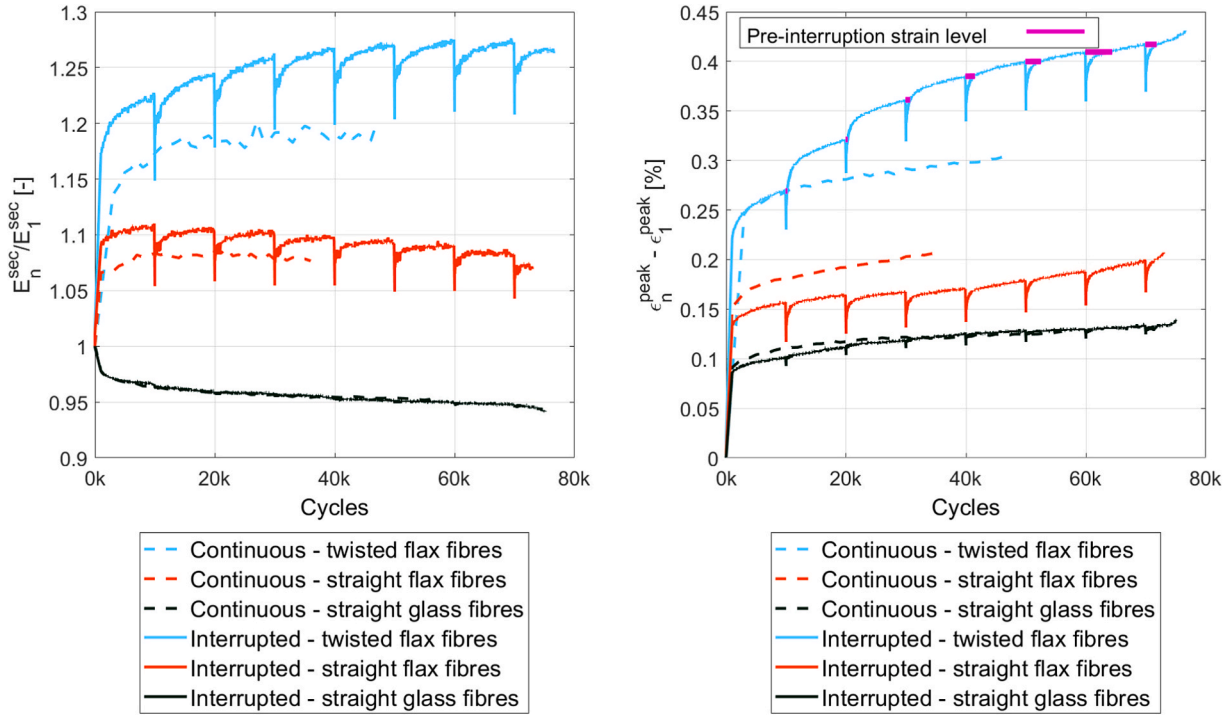

Fig. 20. Typical modulus evolution (left) and strain accumulation (right) during continuous and interrupted fatigue testing. Each colour pair (dashed and solid) represents one of the three distinct laminate configurations investigated, selected based on similar fatigue life.

Table 4
Results of continuous fatigue vs interrupted fatigue. Mean and standard deviation in bold.

		Fatigue life [k]				Ultimate strain [%]			
		Sample			mean ± stdv	Sample			mean ± stdv
		1	2	3		1	2	3	
Straight glass fibres	**Continuous**	48	57	192	**99 ± 81**	1.20	1.20	1.23	**1.21 ± 0.02**
	Interrupted	54	75	150	**93 ± 50**	1.26	1.21	1.26	**1.24 ± 0.03**
Straight flax fibres	**Continuous**	36	57	168	**87 ± 71**	1.08	1.02	0.93	**1.01 ± 0.08**
	Interrupted	24	73	136	**78 ± 56**	1.19	1.05	0.96	**1.07 ± 0.12**
Twisted flax yarns	**Continuous**	47	55	82	**61 ± 18**	1.30	1.29	1.35	**1.31 ± 0.03**
	Interrupted	77	118	122	**105 ± 25**	1.55	1.45	1.49	**1.50 ± 0.05**

Table 5
Estimated contribution of strain recovery to the extension of fatigue life in twisted flax yarn reinforced laminates under interrupted loading.

Fatigue cycles to retrieve pre-interruption strain accumulation													
Block number	2	3	4	5	6	7	8	9	10	11	12	13	Total
Sample 1	200	283	707	1′500	2′500	4′400	1′800	–	–	–	–	–	11 k
Sample 2	0	4′900	5′800	4′000	5′700	1′700	1′400	4′800	6′400	4′800	2′800	–	42 k
Sample 3	2′200	2′000	3′700	3′700	2′400	3′300	2′700	3′000	4′300	4′000	4′000	1′300	37 k

pre-existing cracks without significant additional crack growth until flax fibres accumulate strain equivalent to their pre-interruption level, thereby extending fatigue life. This extension of fatigue life, based on the assumption of crack retardation, is computed for the samples shown in Fig. 20 (pink lines) and two other samples from the same laminate tested with the same conditions. Table 5 shows the number of cycles during which the accumulated strain remained below the pre-interruption level for each loading block and the sum for the entire life. This sum over the 3 specimens tested suggests that strain recovery contributes to an average extension of fatigue life by approximately 30′000 cycles, which aligns well with the experimentally observed increase reported in Table 4. Specifically, the average fatigue life is observed to increase from 61′000 to 105′000 cycles. Furthermore, an increase in the ultimate strain from 1.31 % to 1.50 % (as shown in Table 4) is also noted. This increase in ultimate strain may facilitate additional damage accumulation and propagation prior to failure, thereby further contributing to the extension of fatigue life.

In summary, the effects of loading interruptions on the fatigue response of flax FRP composites are strongly influenced by the viscoelastic nature of the fibre and preform microstructure. While the predominantly UD elastic glass fibre laminate remains largely unaffected by loading interruptions, both flax-based laminates exhibit pronounced sensitivity, characterised by stiffness reductions and partial strain recovery during unloading periods. The twisted flax yarn laminate, in particular, demonstrates a notable enhancement in fatigue life and ultimate strain, which is hypothesised to be attributed to a viscoelastic strain recovery and potential intra-yarn crack closure phenomena. These mechanisms appear to mitigate damage progression during interruptions, effectively reducing the number of damaging cycles and promoting delayed failure.

4. Conclusion

The effects of pre-straining, pre-creeping, and fatigue interruptions (auxiliary loading sequences) on the fatigue performance of flax FRPs $[0/90/0]_S$ laminates were investigated. Performance was assessed through stiffness evolution, strain accumulation, fatigue life, and benchmarked against [0/90/0] glass FRP laminates. The effects of microstructural re-arrangement at fibre/yarn levels were scrutinised by investigating fatigue performance of $[0/90/0]_S$ flax FRP/epoxy laminates reinforced with both straight fibres (UD flax tape), and twisted yarns (Amplitex). The effect of microstructure of the laminate on fatigue performance was further investigated by damage patterns analysis employing optical microscopy and X-ray tomography. The following conclusions can be drawn:

Influence of pre-loading and load interruptions:

- The fatigue performance of glass FRP laminates was minimally influenced by auxiliary loading sequences (preloading and load interruptions), whereas flax FRP laminates exhibited significant sensitivity. This disparity was attributed to the intrinsic complex microstructure and viscoplasticity of flax fibres.
- Pre-creeping markedly enhanced the fatigue performance of $[0/90/0]_S$ flax FRPs, especially those with twisted yarns, yielding a near elimination of strain accumulation, a 32 % increase in secant modulus, and a 3-fold increase in fatigue life. Pre-straining was also found to improve fatigue performance but was less effective than pre-creeping.
- Intermittent fatigue loading improved the fatigue life by 70 % in twisted-yarn laminates and was linked to strain recovery, suggesting that continuous fatigue testing may yield conservative estimates for realistic intermittent loading scenarios. No trend exceeding the inherent scatter in fatigue life data was observed in straight flax fibre and straight glass fibre laminates.

Influence of microstructure:

- The quasi-static and fatigue test results of laminates reinforced with straight fibres (UD FlaxTape) exhibited greater scatter compared to those with twisted yarn preform (Amplitex). This larger scatter is attributed to the inhomogeneous areal density of the UD FlaxTape, leading to possible variation in fibre volume fraction between specimens, hence a larger variation in mechanical properties.
- Laminates reinforced with twisted yarns exhibited approximately double the fatigue-induced stiffening and strain accumulation compared to straight-fibre laminates.
- Stiffness degradation in $[0/90/0]_S$ laminates with straight flax fibres was associated with transverse matrix cracks in the 90° plies. In contrast, the absence of stiffness degradation in laminates with twisted yarns was attributed to crack confinement within the yarns.
- The greater stiffening effect observed in laminates with twisted flax yarns compared to straight flax fibre laminates (32 % vs. 12 %) was partly attributed to the helical yarn architecture, which resists volumetric deformation and thereby enhances stiffness beyond the sole contribution of fibre angle alignment.

CRediT authorship contribution statement

Valentin Perruchoud: Writing – original draft, Visualization, Investigation, Formal analysis, Data curation, Conceptualization, Methodology. **René Alderliesten:** Writing – review & editing, Supervision, Methodology. **Yasmine Mosleh:** Conceptualization, Methodology, Writing - original draft, Writing – review & editing, Supervision, Funding acquisition.

Declaration of competing interest

The authors declare that they have no known competing financial interests or personal relationships that could have appeared to influence the work reported in this paper.

Acknowledgments

The authors express their gratitude to Alexandros Prapavesis in the Composites Materials Group at KU Leuven for performing the micro-CT scans and processing the data to generate the micro-CT images presented in this study.

Data availability

Data will be made available on request.

References

[1] A. Sayyidmousavi et al., 'The Role of Viscoelasticity on the Fatigue of Angle-ply Polymer Matrix Composites at High and Room Temperatures- A Micromechanical Approach', *Appl Compos Mater*, vol. 22, no. 3, pp. 307–321, Jun. 2015 [Online]. Available: 10.1007/s10443-014-9409-0.

[2] A. Movahedirad et al., 'Creep-fatigue interaction in composite materials', presented at the 17th European Conference on Composite Materials, 2016[Online]. Availablehttps://infoscience.epfl.ch/handle/20.500.14299/126539[Accessed: 13March2025].

[3] R. M. Guedes, 'Durability of polymer matrix composites: Viscoelastic effect on static and fatigue loading', *Composites Science and Technology*, vol. 67, no. 11, pp. 2574–2583, Sep. 2007 [Online]. Available: 10.1016/j.compscitech.2006.12.004.

[4] J. Petermann and K. Schulte, 'The effects of creep and fatigue stress ratio on the long-term behaviour of angle-ply CFRP', *Composite Structures*, vol. 57, no. 1, pp. 205–210, Jul. 2002 [Online]. Available: 10.1016/S0263-8223(02)00084-3.

[5] B. Vieille et al., 'About the creep-fatigue interaction on the fatigue behaviour of off-axis woven-ply thermoplastic laminates at temperatures higher than *Tg*', *Composites Part B: Engineering*, vol. 58, pp. 478–486, Mar. 2014 [Online]. Available: 10.1016/j.compositesb.2013.11.005.

[6] W. Claassen and G. Zarifis, 'First Bio-Based Composite Movable Bicycle Bridge', *Structural Engineering International*, vol. 31, no. 2, pp. 227–232, Apr. 2021 [Online]. Available: 10.1080/10168664.2020.1840945.

[7] A. V. Movahedi-Rad et al., 'Interrupted tension-tension fatigue behavior of angle-ply GFRP composite laminates', *International Journal of Fatigue*, vol. 113, pp. 377–388, Aug. 2018 [Online]. Available: 10.1016/j.ijfatigue.2018.05.001.

[8] V. Keryvin et al., 'Analysis of flax fibres viscoelastic behaviour at micro and nano scales', *Composites Part A: Applied Science and Manufacturing*, vol. 68, pp. 219–225, Jan. 2015 [Online]. Available: 10.1016/j.compositesa.2014.10.006.

[9] L. Pupure et al., 'Development of constitutive model for composites exhibiting time dependent properties', *IOP Conf. Ser.: Mater. Sci. Eng.*, vol. 48, no. 1, p. 012007, Dec. 2013 [Online]. Available: 10.1088/1757-899X/48/1/012007.

[10] M. Abida et al., 'A viscoelastic–viscoplastic model with hygromechanical coupling for flax fibre reinforced polymer composites', *Composites Science and Technology*, vol. 189, p. 108018, Mar. 2020 [Online]. Available: 10.1016/j.compscitech.2020.108018.

[11] C. Wang et al., 'Investigation of Microfibril Angle of Flax Fibers Using X-Ray Diffraction and Scanning Electron Microscopy', *Journal of Natural Fibers*, vol. 17, pp. 1–10, Nov. 2018 [Online]. Available: 10.1080/15440478.2018.1546639.

[12] A. Bourmaud et al., 'Relationships between micro-fibrillar angle, mechanical properties and biochemical composition of flax fibers', *Industrial Crops and Products*, vol. 44, pp. 343–351, Jan. 2013 [Online]. Available: 10.1016/j.indcrop.2012.11.031.

[13] O. M. Astley and A. M. Donald, 'A small-angle X-ray scattering study of the effect of hydration on the microstructure of flax fibers', *Biomacromolecules*, vol. 2, no. 3, pp. 672–680, 2001 [Online]. Available: 10.1021/bm005643l.

[14] M. Müller et al., 'Combined X-ray microbeam small-angle scattering and fibre diffraction experiments on single native cellulose fibres', *Journal of Applied Crystallography - J APPL CRYST*, vol. 33, pp. 817–819, Jun. 2000 [Online]. Available: 10.1107/S0021889800099751.

[15] Z. Zhang et al., 'High performances of plant fiber reinforced Composites—A new insight from hierarchical microstructures', *Composites Science and Technology*, vol. 194, p. 108151, Apr. 2020 [Online]. Available: 10.1016/j.compscitech.2020.108151.

[16] C. Wang et al., 'Investigation of Microfibril Angle of Flax Fibers Using X-Ray Diffraction and Scanning Electron Microscopy', *Journal of Natural Fibers*, vol. 17, no. 7, pp. 1001–1010, Jul. 2020 [Online]. Available: 10.1080/15440478.2018.1546639.

[17] *Direct Observation of Microfibril Arrangement in a Single Native Cellulose Fiber by Microbeam Small-Angle X-ray Scattering | Macromolecules*. [Online]. Available: https://pubs.acs.org/doi/10.1021/ma980004c. [Accessed: 24 Dec. 2024].

[18] E. Richely et al., 'Influence of defects on the tensile behaviour of flax fibres: Cellulose microfibrils evolution by synchrotron X-ray diffraction and finite element modelling', *Composites Part C: Open Access*, vol. 9, p. 100300, Oct. 2022 [Online]. Available: 10.1016/j.jcomc.2022.100300.

[19] S. Goutianos and T. Peijs, 'The Optimisation of Flax Fibre Yarns for the Development of High-Performance Natural Fibre Composites', *Advanced Composites Letters*, vol. 12, no. 6, p. 096369350301200602, Nov. 2003 [Online]. Available: 10.1177/096369350301200602.

[20] J. Baets et al., 'Determination of the optimal flax fibre preparation for use in unidirectional flax–epoxy composites', *Journal of Reinforced Plastics and Composites*, vol. 33, no. 5, pp. 493–502, Mar. 2014 [Online]. Available: 10.1177/0731684413518620.

[21] Perruchoud V, et al. Pre-straining as an effective strategy to mitigate ratcheting during fatigue in flax FRP composites for structural applications. Heron Feb. 2024; 68.

[22] M. Lu and A. W. Vuure, 'Improving moisture durability of flax fibre composites by using non-dry fibres', *Composites Part A: Applied Science and Manufacturing*, vol. 123, May 2019 [Online]. Available: 10.1016/j.compositesa.2019.05.029.

[23] M. O. Cadavid et al., 'Experimental Studies of Stiffness Degradation and Dissipated Energy in Glass Fibre Reinforced Polymer Composite under Fatigue Loading', *Polymers and Polymer Composites*, vol. 25, no. 6, pp. 435–446, Jul. 2017 [Online]. Available: 10.1177/096739111702500602.

[24] K. S. Ravi Chandran, 'Review: Fatigue of Fiber-Reinforced Composites, Damage and Failure', *J Indian Inst Sci*, vol. 102, no. 1, pp. 439–460, Jan. 2022 [Online]. Available: 10.1007/s41745-021-00280-y.

[25] Y. Zhao et al., 'A Fatigue Damage Model for FRP Composite Laminate Systems Based on Stiffness Reduction', *SDHM*, vol. 13, no. 1, pp. 85–103, 1970 [Online]. Available: 10.32604/sdhm.2019.04695.

[26] C. Baley, 'Analysis of the flax fibres tensile behaviour and analysis of the tensile stiffness increase', *Composites Part A-applied Science and Manufacturing - COMPOS PART A-APPL SCI MANUF*, vol. 33, pp. 939–948, Jul. 2002 [Online]. Available: 10.1016/S1359-835X(02)00040-4.

[27] S. Liang et al., 'A comparative study of fatigue behaviour of flax/epoxy and glass/epoxy composites', *Composites Science and Technology*, vol. 72, pp. 535–543, Mar. 2012 [Online]. Available: 10.1016/j.compscitech.2012.01.011.

[28] S. Liang et al., 'Properties evolution of flax/epoxy composites under fatigue loading', *International Journal of Fatigue*, vol. 63, pp. 36–45, Jun. 2014 [Online]. Available: 10.1016/j.ijfatigue.2014.01.003.

[29] T. Jeannin et al., 'Influence of hydrothermal ageing on the fatigue behaviour of a unidirectional flax-epoxy laminate', *Composites Part B: Engineering*, vol. 174, p. 107056, Oct. 2019 [Online]. Available: 10.1016/j.compositesb.2019.107056.

[30] L. Nuez et al., 'Exploring the effect of relative humidity on dynamic evolution of flax fibre's microfibril angle through in situ tensile tests under synchrotron X-ray diffraction', *Industrial Crops and Products*, vol. 188, p. 115592, Nov. 2022 [Online]. Available: 10.1016/j.indcrop.2022.115592.

[31] E. Richely et al., 'Measurement of microfibril angle in plant fibres: Comparison between X-ray diffraction, second harmonic generation and transmission ellipsometry microscopies', *Composites Part C: Open Access*, vol. 11, p. 100355, Jul. 2023 [Online]. Available: 10.1016/j.jcomc.2023.100355.

[32] F. Bensadoun et al., 'Fatigue behaviour assessment of flax–epoxy composites', *Composites Part A: Applied Science and Manufacturing*, vol. 82, pp. 253–266, Mar. 2016 [Online]. Available: 10.1016/j.compositesa.2015.11.003.

[33] M. Abida et al., 'Inverse approach for flax yarns mechanical properties identification from statistical mechanical characterization of the fabric', *Mechanics of Materials*, vol. 151, p. 103638, Dec. 2020 [Online]. Available: 10.1016/j.mechmat.2020.103638.

[34] M. Rask and B. Madsen, 'Twisting of fibres in yarns for natural fibre composites', 2011[Online]. Availablehttps://www.semanticscholar.org/paper/Twisting-of-fibres-in-yarns-for-natural-fibre-Rask-Madsen/fc5e290d30bb051e79f89d930ef5f82b8a75102d[Accessed: 4November2024].

[35] J. W. S. Hearle, 'The fine structure of fibers and crystalline polymers. III. Interpretation of the mechanical properties of fibers', *Journal of Applied Polymer Science*, vol. 7, no. 4, pp. 1207–1223, 1963 [Online]. Available: 10.1002/app.1963.070070403.

[36] S. Liang et al., 'A comparative study of fatigue behaviour of flax/epoxy and glass/epoxy composites', *Composites Science and Technology*, vol. 72, no. 5, pp. 535–543, Mar. 2012 [Online]. Available: 10.1016/j.compscitech.2012.01.011.

[37] D. U. Shah, 'Damage in biocomposites: Stiffness evolution of aligned plant fibre composites during monotonic and cyclic fatigue loading', *Composites Part A: Applied Science and Manufacturing*, vol. 83, pp. 160–168, Apr. 2016 [Online]. Available: 10.1016/j.compositesa.2015.09.008.

[38] F. K. Sodoke et al., 'Hygrothermal effects on fatigue behavior of quasi-isotropic flax/epoxy composites using principal component analysis', *J Mater Sci*, vol. 51, no. 24, pp. 10793–10805, Dec. 2016 [Online]. Available: 10.1007/s10853-016-0291-z.

[39] P. M. Giuliani et al., 'Characterizing flax fiber reinforced bio-composites under monotonic and cyclic tensile loading', *Composite Structures*, vol. 280, p. 114803, Jan. 2022 [Online]. Available: 10.1016/j.compstruct.2021.114803.

[40] A. Moghimi-ardekani et al., 'Damage indicators in unidirectional natural fibre composites under fatigue loading', *Composite Structures*, vol. 349–350, p. 118522, Dec. 2024 [Online]. Available: 10.1016/j.compstruct.2024.118522.

[41] V. Perruchoud et al., 'Enhancing fatigue performance of structural biocomposites by pre-straining and pre-creeping methods', in *Proceedings of the 21st European Conference on Composite Materials*, Nantes, France, 2024, vol. Volume 3-Material and Structural Behavior – Simulation&Testing, pp. 1490–1498.